



CHORUS

This is the accepted manuscript made available via CHORUS. The article has been published as:

Superconductivity-localization interplay and fluctuation magnetoresistance in epitaxial $\text{BaPb}_{1-x}\text{Bi}_x\text{O}_3$ thin films

D. T. Harris, N. Campbell, R. Uecker, M. Brützam, D. G. Schlom, A. Levchenko, M. S. Rzchowski, and C.-B. Eom

Phys. Rev. Materials **2**, 041801 — Published 16 April 2018

DOI: [10.1103/PhysRevMaterials.2.041801](https://doi.org/10.1103/PhysRevMaterials.2.041801)

Superconductivity-localization interplay and fluctuation magnetoresistance in epitaxial $\text{BaPb}_{1-x}\text{Bi}_x\text{O}_3$ thin films

D.T. Harris,¹ N. Campbell,² R. Uecker,³ M. Brützmam,³ D.G. Schlom,^{4,5} A. Levchenko,² M.S. Rzchowski,² and C.-B. Eom^{1,*}

¹*Department of Materials Science and Engineering,*

University of Wisconsin-Madison, Madison, WI 53706, USA

²*Department of Physics, University of Wisconsin-Madison, Madison, WI 53706, USA*

³*Leibniz Institute for Crystal Growth, Berlin, Germany*

⁴*Department of Materials Science and Engineering,*

Cornell University, Ithaca, NY 14853, USA

⁵*Kavli Institute at Cornell for Nanoscale Science, Ithaca, NY 14853, USA*

(Dated: April 2, 2018)

Abstract

$\text{BaPb}_{1-x}\text{Bi}_x\text{O}_3$ is a superconductor, with transition temperature $T_c = 11$ K, whose parent compound BaBiO_3 possess a charge ordering phase and perovskite crystal structure reminiscent of the cuprates. The lack of magnetism simplifies the $\text{BaPb}_{1-x}\text{Bi}_x\text{O}_3$ phase diagram, making this system an ideal platform for contrasting high- T_c systems with isotropic superconductors. Here we use high-quality epitaxial thin films and magnetotransport to demonstrate superconducting fluctuations that extend well beyond T_c . For the thickest films (thickness above ~ 100 nm) this region extends to ~ 27 K, well above the bulk T_c and remarkably close to the higher T_c of $\text{Ba}_{1-x}\text{K}_x\text{BiO}_3$ ($T_c = 31$ K). We drive the system through a superconductor-insulator transition by decreasing thickness and find the observed T_c correlates strongly with disorder. This material manifests strong fluctuations across a wide range of thicknesses, temperatures, and disorder presenting new opportunities for understanding the precursor of superconductivity near the 2D-3D dimensionality crossover.

In contrast to the layered cuprate superconductors, $\text{BaPb}_{1-x}\text{Bi}_x\text{O}_3$ (BPBO, $T_c = 11$ K) and $\text{Ba}_{1-x}\text{K}_x\text{BiO}_3$ (BKBO, $T_c = 31$ K) are isotropic and nonmagnetic, however, there are still interesting similarities^{1,2}. The bismuthates are complex oxides with oxygen octahedra similar to the cuprates, and the parent insulating BaBiO_3 (BBO) possesses a competing phase, a charge density wave (CDW), which is suppressed for superconducting compositions. The study of the simpler, conventional bismuthate may lead to a deeper understanding of the role of CDW physics in the more complicated cuprates. The cuprate phase diagram is characterized by numerous electronic and magnetic phases and the properties are strongly influenced by disorder³. In thin conventional superconductors, disorder can lead to a pseudogap reminiscent of the high- T_c cuprates, suggesting a possible connection between the layered cuprate structure and dimensionally confined conventional superconductors⁴. In superconducting BPBO single crystals, Luna *et al.*⁵ found a reduction in the density of states consistent with a disorder-driven metal-insulator transition and predicted a disorder-free T_c of 17 K in the strong coupling limit and 52 K in the weak coupling limit for $x = 0.25$.

Here we demonstrate an extended region of positive magnetoresistance in epitaxial thin films of $\text{BaPb}_{0.75}\text{Bi}_{0.25}\text{O}_3$ that is well described by superconducting fluctuations. This fluctuation regime persists for the thickest films that are well within the 3D regime, consistent with the high disorder found in our films. Restricting film thickness causes a superconductor-to-insulator transition (SIT) that correlates with disorder. Although our results are consistent with the disorder levels found in bulk single crystals⁵, we find that the critical thickness for superconductivity depends on extrinsic factors related to the poor lattice matching of BPBO with common perovskite substrates.

The high-quality epitaxial growth of BBO-based materials presents additional challenges since B(K,Pb)BO exhibits one of the largest lattice parameters ($a_{pc} = 4.26 - 4.36$ Å) among the ABO_3 perovskites. There is little understanding of how the large lattice mismatch, $> 10\%$ on typical commercial perovskite substrates such as SrTiO_3 (STO), impacts the structural and electronic properties of these materials. Reports in the literature demonstrate epitaxial growth on STO⁶⁻⁸, MgO ($a = 4.21$ Å)⁹⁻¹¹, or by using buffer layers¹². We use recently developed LaLuO_3 (LLO, $a_{pc} = 4.187$ Å) single crystals¹³ as a substrate to grow BPBO ($x = 0.25, a_{pc} = 4.29$ Å) and BBO films, demonstrating that reduction of the lattice mismatch from $\sim 10.1\%$ (STO) to $\sim 2.7\%$ (LLO) improves crystallinity, surface roughness, and superconducting transitions.

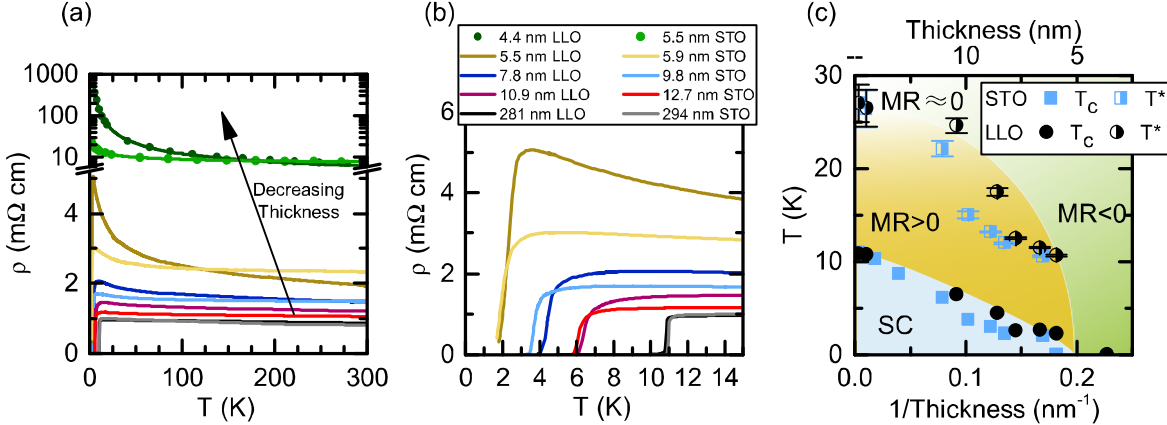


FIG. 1: Resistivity measurements from 300 K to 2 K. (a) Representative resistivity measurements for films on LLO and STO. For 4.4 nm on LLO and 5.5 nm on STO, the dots are experimental data and the solid line is a fit to a variable range hopping model. (b) Transition region for superconducting samples from (a). (c) Phase diagram of the BPBO system vs thickness for films on LLO (black circles) and STO (blue squares). The shaded regions are guides to the eye.

Epitaxial films of optimally doped $x = 0.25$ BPBO were grown using 90° off-axis rf-magnetron sputtering on (001) STO and (110) LLO substrates (see Supplemental Material for detailed methods). Thick films grown on both substrates exhibit a room temperature resistivity of $0.8\text{m}\Omega\text{-cm}$, the lowest reported for BPBO with $x = 0.25$, and a slightly negative $d\rho/dT$ typical for optimally doped BPBO, as seen in Fig. 1^{7,14,15}. The thick films exhibit sharp transitions with transition widths of 0.2 K (90%–10% of normal state) and T_c (50% of normal state) of 10.9 K, comparable to bulk single crystal¹⁶ and polycrystalline ceramics¹⁴, and the highest reported for thin films⁷. We also find no evidence of inhomogeneous transitions as seen in bulk single crystals¹⁶. The quality of BPBO films is further demonstrated in Figs. 2(a)-2(c) by the narrow ω -rocking curves, presence of Kiessig fringes, and out-of-plane lattice constant of 4.276 \AA , in good agreement with the bulk value.

Decreasing the film thickness leads to higher resistivity, more negative $d\rho/dT$, depressed T_c , and broadened transitions as shown in Figs. 1(a) and 1(b). The thinnest films on both LLO and STO show insulating behavior well fit by a 2D variable range hopping model ($T_0 = 1070 \text{ K}$ and 7.5 K respectively) over the entire temperature range [solid lines in Fig. 1(a)]. The LLO films exhibit higher T_c when compared with films grown on STO. Fig. 1(c) shows the extracted T_c (50% of normal state), showing a smaller critical thickness for films

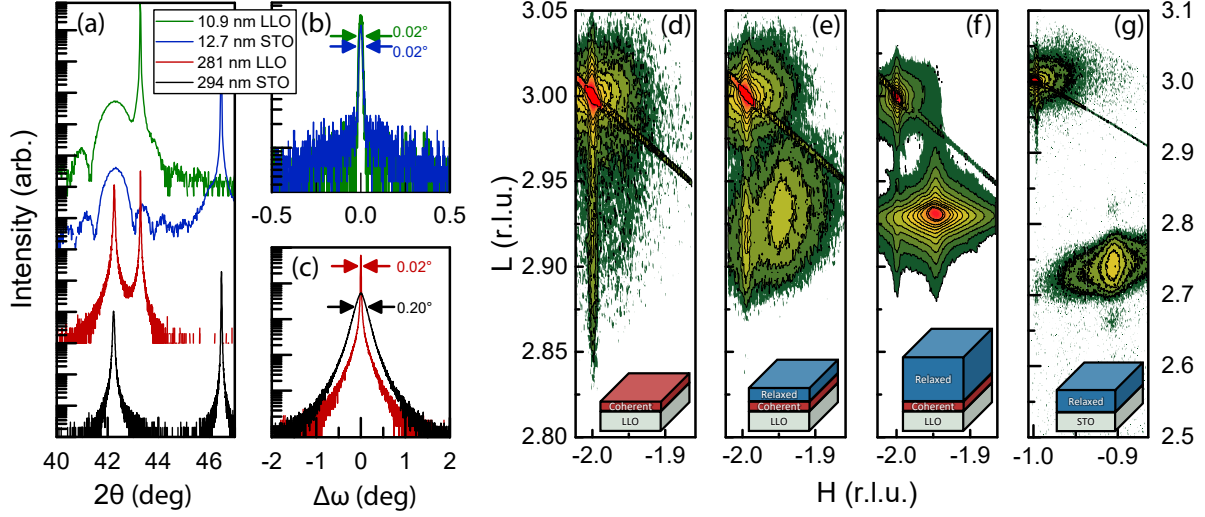


FIG. 2: X-ray diffraction characterization. (a) Representative out of plane $2\theta - \omega$ scans around the 002_{pc} peak for thin (~ 11 nm) and thick (~ 290 nm) BPBO films on STO and LLO. The corresponding rocking curves around the 002_{pc} film peaks for (b) thin and (c) thick films with the full width at half maxes indicated. Reciprocal space maps around the 103_{pc} reflection for (d) a fully coherent 4.4 nm thick film on LLO, as well bilayer relaxed films on LLO (e) 7.8 nm thick and (f) 281 nm thick and (g) fully relaxed 8.2 nm on STO. The inset cartoons show the film structure for each space map.

on LLO ($d_c \sim 5$ nm) than those on STO ($d_c \sim 5.5$ nm).

Previous reports of BPBO polycrystalline films found significant suppression of T_c already apparent at 200 nm, a much larger thickness than the onset of T_c reduction in our epitaxial films¹⁷. Grain boundaries in polycrystalline BPBO form Josephson junctions^{18,19}, leading to reentrant behavior²⁰. Our epitaxial films do not show reentrant behavior, and the high crystalline quality evident in the rocking curves makes the existence of a granular structure unlikely.

Disorder can be parameterized using the Mott-Ioffe-Regel parameter, $k_F l$, determined from the normal state resistivity ρ and the Hall coefficient R_H by using the free electron formula $k_F l = (3\pi^2)^{2/3} \hbar R_H^{1/3} / (\rho e^{5/3})$, which describes the limit of scattering in a system before localization occurs. In our system we find strong correlation between $k_F l$ and T_c , as shown in Fig. 3, with films on LLO showing higher $k_F l$ for a given thickness. The disorder-induced superconductor-insulator transition, controlled by a variety of parameters including

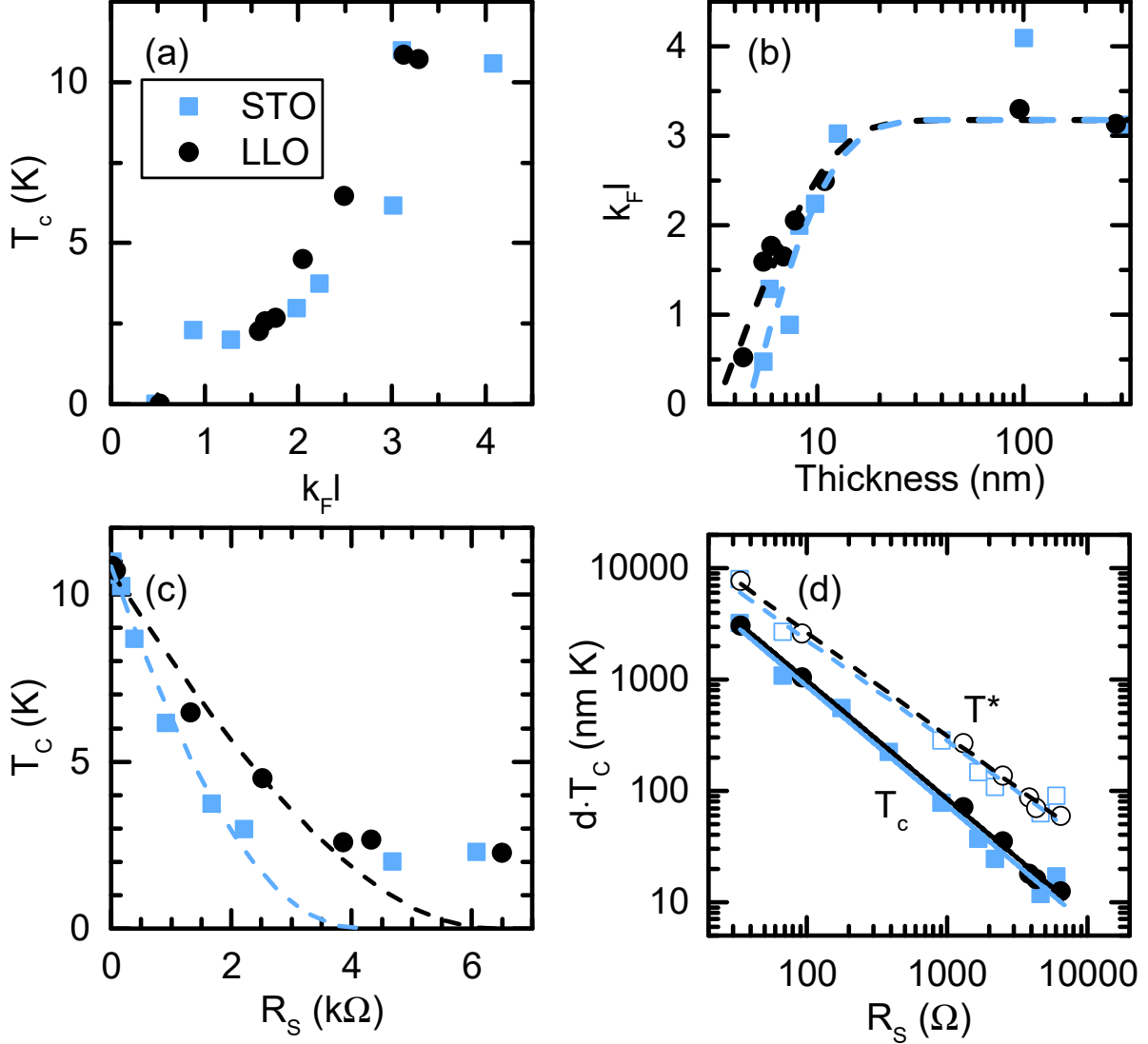


FIG. 3: Disorder and superconductivity. (a) Transition temperature vs. the Mott-Ioffe-Regel parameter, k_{Fl} , (extracted from room temperature measurements), and (b) k_{Fl} vs. thickness (the dashed lines are guides for the eye). (c) T_c vs. the sheet resistance at 20 K. The dashed lines are fits to Finkel'stein's model for a homogenously disordered superconductor. (d) Power-law scaling dependence of thickness times transition temperature ($d \cdot T_c$) versus R_S based on the phenomenological formula $d \cdot T_c = A R_S^{-B}$, where A and B are fitting parameters³¹.

thickness, has been extensively studied in conventional and high-temperature systems, with recent efforts focusing on the quantum nature of the SIT, however, no complete theoretical understanding exists for the variety of phenomena experimentally observed^{20,21}.

For 2D homogeneously disordered films, Finkel'stein developed a model for T_c suppression

from Coulomb interactions assuming no change to the bulk electron gas properties with changes to R_S ²². The data for both sets of films initially fit well to Finkel'stein's model, Fig. 3(c), indicating an increase in the scattering time for films on LLO compared to STO, however, the model breaks down for films close to the critical thickness. Epitaxial films can experience thickness dependent strain relaxation, resulting in changes to material structure and properties with decreasing thickness. We investigate the strain state of our films using reciprocal space maps, shown in Fig. 2(d)-2(g). On STO, BPBO grows relaxed, as reported by other groups^{23,24}. On LLO, we obtain coherent growth for films up to ~ 4.5 nm, with an abrupt relaxation at ~ 4.5 nm that forms a layered structure [see inset schema Figs. 2(d)-2(f)] that remains present for the thickest films studied. Similar relaxation behavior has been reported for other oxide epitaxial systems²⁵⁻²⁸ and occurs in undoped BaBiO₃ films as shown in supplemental Fig. 1 of Ref.²⁹. The relaxed BPBO phase on both substrates has lattice constants of $a_{pc} = 4.29$ Å and $c_{pc} = 4.28$ Å, in good agreement with bulk values from powder diffraction³⁰. Films on both substrates show variations in the out-of-plane lattice parameter at low thicknesses, see supplemental Fig. 2 in Ref.²⁹, indicating assumptions are likely violated for the Finkel'stein model. Both sets of films show a power law relationship between $d \cdot T_c$ and R_S , shown in Fig. 3(d), an empirical observation found in many thin superconducting systems that is not well understood theoretically³¹.

The x-ray diffraction in Fig. 2 reveals rocking curves with higher diffuse backgrounds and RSMs with broader in-plane components for all films grown on STO. The mosaic spread seen in the broadening of rocking curves and reciprocal space maps is indicative of a high dislocation density^{32,33}. Improving the film-substrate lattice match by switching to LLO reduces the diffuse background, consistent with a reduction in dislocations and mosaicity. Additionally, surface and interface scattering become more important in thinner films and atomic force microscopy (AFM) consistently reveals smoother surfaces for films grown on LLO, as shown in Fig. 4. The smaller critical thickness for superconductivity for films on LLO is consistent with the reduced disorder in the higher quality, smoother films³⁴⁻³⁶.

Thin disordered superconductors routinely show evidence of superconductivity above the measured T_c ^{20,37}. We investigated the insulating to superconducting transition via magnetotransport, revealing positive magnetoresistance (MR) in all superconducting films well above T_c . Non-superconducting films (with thickness less than a critical thickness $d_c \sim 5 - 6$ nm) show only negative magnetoresistance that increases in magnitude as the temperature

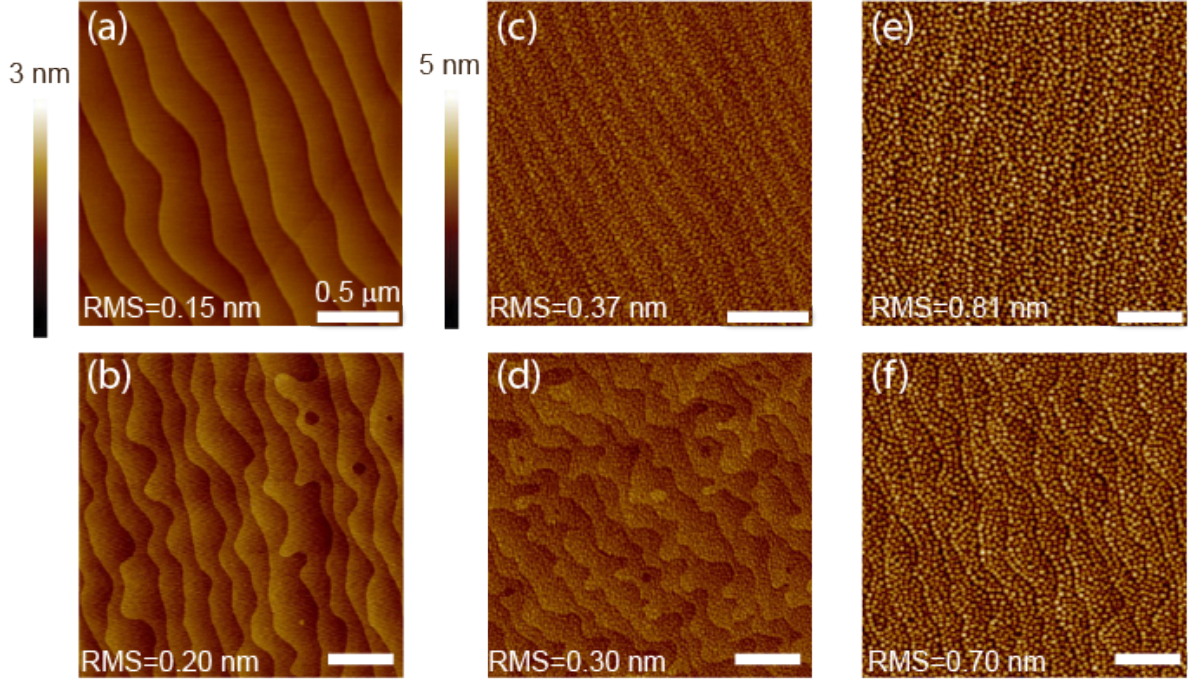


FIG. 4: Atomic force microscopy images. Surface topography images for (a) treated STO and (b) LLO, (c) 12.7 nm BPBO on STO, (d) 10.9 nm on LLO, (e) 101 nm on STO, and (f) 96.5 nm on LLO.

is lowered, as shown in Fig. 5(a) for an insulating film on STO. Magnetoresistance in the insulating phase of disordered superconductors can show a variety of responses. For instance, positive magnetoresistance reported in insulating samples is evidence for existence of localized superconductivity persisting beyond the superconductor-insulator transition^{38,39}. However, the observation of positive magnetoresistance in insulating samples is not universal even within the same material system, suggesting that localization can occur through different mechanisms of disorder resulting in distinct insulator states^{40–43}.

In contrast to the insulating samples, superconducting films show an extended region of positive magnetoresistance above T_c that extends to a temperature T^* that is highly correlated with T_c , as shown in Fig. 5(e), suggesting a strong link between the positive MR and superconductivity^{44–47}. In superconductors, a positive magnetoresistance above T_c is associated with the presence of superconducting fluctuations and can arise from several different mechanisms³⁷. For thin ~ 8 nm films, we fit our experimental MR data to models for fluctuations and weak localization in 2D disordered systems, see supplemental information, and find excellent agreement in the region far above the transition and at low fields, as

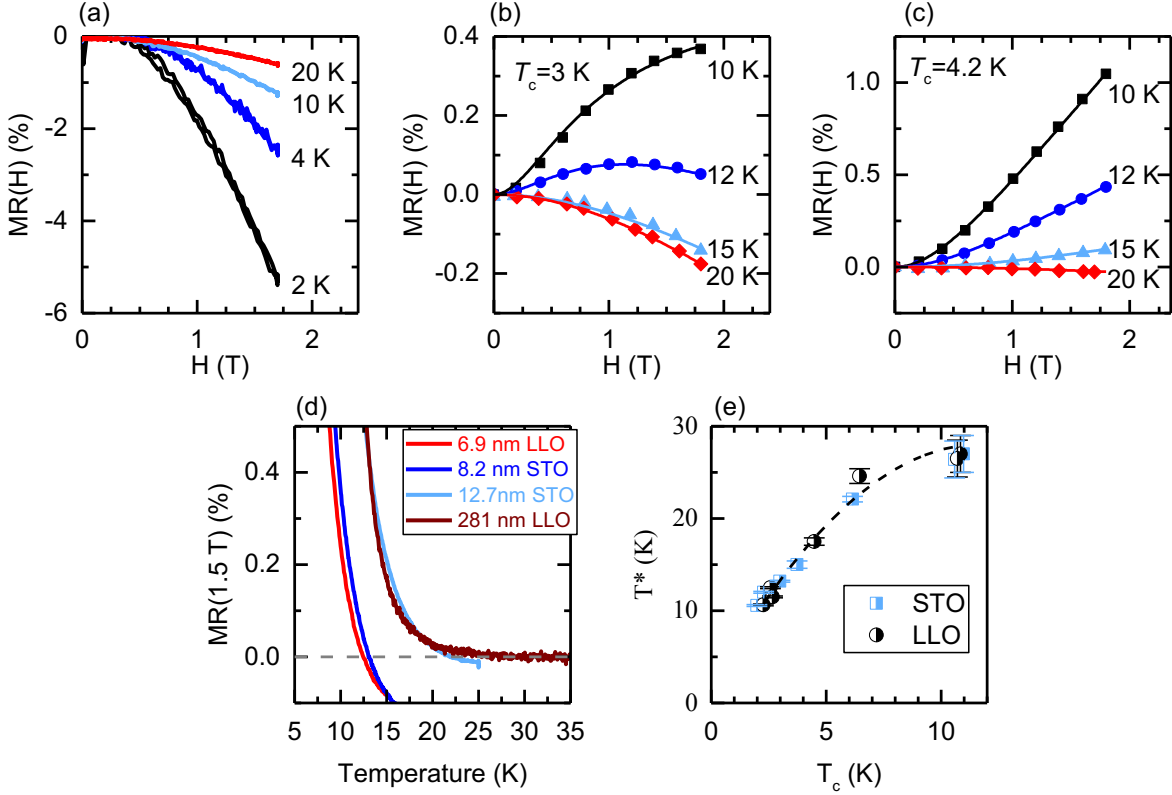


FIG. 5: Magnetoresistance measurements above T_c . Magnetoresistance at fixed temperatures for (a) insulating 5.5 nm on STO, (b) superconducting 8.2 nm BPBO on STO, and (c) superconducting 7.8 nm BPBO on LLO. In (b) and (c) the markers are experimental data points with the solid lines fits to superconducting fluctuations and weak localization in a 2D disordered system. (d) Representative magnetoresistance vs temperature. (e) The MR inflection temperature T^* vs T_c (the dashed line is a guide for the eye).

shown in Figs. 5(b) and 5(c). We note that while we used the readily available expressions for magnetoresistance of a 2D film^{37,48,49} and obtained excellent agreement with experiment, far from T_c we expect a shortened coherence length and that our films are likely in the 3D regime⁵⁰. The theory of fluctuations for 3D systems is incomplete with no expressions for the field dependence for all terms available, in part due to difficulty in preparing metallic systems with high enough disorder for measurable fluctuations⁵¹. The BPBO system exhibits measurable fluctuations across a wide range of thicknesses and at temperatures easily accessed by common *He* cryostats, allowing comparison with theory and study of the cross-over regime from 2D to 3D. Although we are beyond the strict limits of 2D fluctuation

theory, the correlation between T_c and T^* [Fig. 5(e)] and the good fits of experimental data strongly suggest the positive MR originates from superconducting fluctuations. Weak anti-localization (WAL) can also lead to positive MR in systems with strong spin-orbit coupling. Separation of the various terms that contribute to MR is difficult, but we point out the strong correlation between T_c and T^* [Fig. 5(e)], the power-law scaling of T^* in a manner similar to T_c [Fig. 3(d)], and the smooth divergence of MR as T_c is approached [Fig. 5(d)]. Further demonstration of the presence of fluctuations is beyond the scope of the present study but could be searched for in magnetic susceptibility or other above- T_c phenomena³⁷.

We extracted T^* for each film by fixing field and sweeping temperature, as shown in Fig. 5(d), resulting in the phase diagram shown in Fig. 1(c). The existence of fluctuations far above the observed T_c is expected for films approaching the critical thickness for superconductivity⁴⁰, however, surprisingly, the thickest films (100-300 nm) show positive magnetoresistance extending to ~ 27 K (Fig. 5(d)), significantly higher than the bulk transition $T_{c0} = 11$ K. Clean, bulk superconductors are expected to have only a very narrow temperature regime where fluctuations manifest³⁷. The superconducting coherence length of BPBO is ~ 8 nm and isotropic, placing these thick films firmly in the 3D regime^{14,52}. Measurements on single crystals of BPBO reveal scaling consistent with a 2D material¹⁵ and TEM measurements show some evidence of striped polymorph ordering on the scale of the coherence length⁵³, suggesting nanostructuring of the material could contribute to this phenomenon. We, however, have no evidence of such stripes in our films, and our measurements suggest a high level of disorder in BPBO. The Mott-Ioffe-Regel parameter, $k_F l$, extracted from room temperature measurements for the thick films is $\sim 3-4$, consistent with bulk single crystal measurements^{16,52}, and in the regime of a disordered material. This finding agrees with tunneling measurements on bulk BPBO crystals that show changes to the tunneling density of states arising from disorder⁵.

The role of disorder and superconducting fluctuations has interested the community, in part due to the layered structure of the high- T_c cuprates and nearby insulating phases that promote the presence of fluctuations. Similarly, thin conventional superconductors exhibit strong fluctuations, proximity to a superconductor-insulator transition, and evidence for a pseudo-gap in the density of states, suggesting a connection between thin conventional superconductors and the higher- T_c layered materials⁴. Disordered NbN films exhibit magnetoresistance inflection at temperatures close to the where the energy gap from scanning

tunneling spectroscopy vanishes³⁹. There is one report of a pseudogap in $\text{Ba}_{0.67}\text{K}_{0.33}\text{BiO}_3$ ⁵⁴ and a pseudogap has been suggested for BPBO⁵⁵, however, experimentally the normal state properties are poorly explored in BBO superconductors.

Although the physical origin of disorder in BPBO is as of yet undetermined, there are several possibilities. Optical and terahertz spectroscopy measurements hint at local CDW fluctuations that could compete with superconductivity prior to the onset of a semiconducting bandgap from a long-range CDW^{56,57}. In BPBO there is also evidence that many samples consist of two structural polymorphs, tetragonal and orthorhombic, and that superconductivity is correlated with the tetragonal volume fraction^{30,58}. Our measured T^* of ~ 27 K in thick films is very close to the higher T_c of $\text{Ba}_{1-x}\text{K}_x\text{BiO}_3$, and in reasonable agreement with the prediction for disorder-free BPBO from Luna *et al.*⁵. The similar temperature scales of our T^* , the disorder free T_c prediction, and the onset of CDW fluctuations strongly suggests a connection of these phenomenon. Models of T_c suppression, such as the Finkel'stein model, do not consider effects such as a competing CDW phase. The surprisingly large temperature range with measurable fluctuation effects are consistent with BPBO possessing a significantly higher T_c that is obscured by disorder.

Our work demonstrates a smaller critical thickness for films grown on LLO, however the lattice mismatch is still large compared to other perovskite heterostructures, preventing growth of films thick enough to study epitaxial strain engineering^{59,60}. Further improvements in crystalline and interface qualities are important for BBO heterostructures that could use thin layers to control the CDW²³ or interface superconducting BPBO with the predicted topological insulating phase of BBO⁶¹. Our results show how extrinsic contributions related to material limitations play an important role in the ultra-thin limit, as well as reveal new above- T_c phenomenon in BPBO.

Acknowledgements

Synthesis, characterization, and analysis were supported with funding from the Department of Energy Office of Basic Energy Sciences under award number DE-FG02-06ER46327. The theoretical input of A.L. was supported by NSF CAREER Grant No. DMR-1653661. We thank Art Hebard for helpful discussions and Jim Langyel for assistance with x-ray

diffraction.

-
- * Electronic address: eom@engr.wisc.edu
- ¹ A. W. Sleight, J. L. Gillson, and P. E. Bierstedt, *High-Temperature Superconductivity in the BaPb_{1-x}Bi_xO₃ System*, Solid State Commun. **17**, 27 (1975).
 - ² R. J. Cava, B. Batlogg, J. J. Krajewski, R. Farrow, L. W. Rupp, a. E. White, K. Short, W. F. Peck, and T. Kometani, *Superconductivity near 30 K without copper: the Ba_{0.6}K_{0.4}BiO₃ perovskite*, Nature **332**, 814 (1988).
 - ³ J. C. Phillips, A. Saxena, and A. R. Bishop, *Pseudogaps, dopants, and strong disorder in cuprate high-temperature superconductors*, Rep. Prog. Phys. **66**, 2111 (2003).
 - ⁴ B. Sacépé, C. Chapelier, T. I. Baturina, V. M. Vinokur, M. R. Baklanov, and M. Sanquer, *Pseudogap in a thin film of a conventional superconductor*, Nat. Commun. **1**, 140 (2010).
 - ⁵ K. Luna, P. Giraldo-Gallo, T. Geballe, I. Fisher, and M. Beasley, *Disorder Driven Metal-Insulator Transition in BaPb_{1-x}Bi_xO₃ and Inference of Disorder-Free Critical Temperature*, Phys. Rev. Lett. **113**, 177004 (2014).
 - ⁶ E. S. Hellman, E. H. Hartford, and R. M. Fleming, *Molecular beam epitaxy of superconducting (Rb,Ba)BiO₃*, Appl. Phys. Lett. **55**, 2120 (1989).
 - ⁷ M. Suzuki, *Properties of BaPb_{1-x}Bi_xO₃ as Observed in Single-Crystal Thin Films*, Jpn. J. Appl. Phys. **32**, 2640 (1993).
 - ⁸ N. C. Plumb, D. J. Gawryluk, Y. Wang, Z. Ristić, J. Park, B. Q. Lv, Z. Wang, C. E. Matt, N. Xu, T. Shang, K. Conder, J. Mesot, S. Johnston, M. Shi, and M. Radović, *Momentum-Resolved Electronic Structure of the High-T_c Superconductor Parent Compound BaBiO₃*, Phys. Rev. Lett. **117**, 037002 (2016).
 - ⁹ E. S. Hellman, E. H. Hartford, and E. M. Gyorgy, *Epitaxial Ba_{1-x}K_xBiO₃ films on MgO: Nucleation, cracking, and critical currents*, Appl. Phys. Lett. **58**, 1335 (1991).
 - ¹⁰ P. Prieto, U. Poppe, W. Evers, R. Hojczyc, C. L. Jia, K. Urban, K. Schmidt, and H. Soltner, *In situ production of epitaxial Ba_{1-x}K_xBiO₃ thin films by high-oxygen-pressure RF sputtering*, Phys. C Supercond. **233**, 361 (1994).
 - ¹¹ K. Inumaru, H. Miyata, and S. Yamanaka, *Partial suppression of structural distortion in epitaxially grown BaBiO₃ thin films*, Phys. Rev. B **78**, 132507 (2008).

- ¹² H. G. Lee, Y. Kim, S. Hwang, G. Kim, T. D. Kang, M. Kim, M. Kim, and T. W. Noh, *Double-layer buffer template to grow commensurate epitaxial BaBiO₃ thin films*, APL Mater. **4**, 126106 (2016).
- ¹³ R. Uecker, R. Bertram, M. Brützam, Z. Galazka, T. M. Gesing, C. Guguschev, D. Klimm, M. Klupsch, A. Kwasniewski, and D. G. Schlom, *Large-lattice-parameter perovskite single-crystal substrates*, J. Cryst. Growth **457**, 137 (2017).
- ¹⁴ T. D. Thanh, A. Koma, and S. Tanaka, *Superconductivity in the BaPb_{1-x}Bi_xO₃ System*, in Ten Years Supercond. 1980-1990, edited by H. R. Ott (Springer Netherlands, Dordrecht, 1980), pp. 259–266.
- ¹⁵ P. Giraldo-Gallo, H. Lee, Y. Zhang, M. J. Kramer, M. R. Beasley, T. H. Geballe, and I. R. Fisher, *Field-tuned superconductor-insulator transition in BaPb_{1-x}Bi_xO₃*, Phys. Rev. B **85**, 174503 (2012).
- ¹⁶ P. Giraldo-Gallo, H. Lee, M. R. Beasley, T. H. Geballe, and I. R. Fisher, *Inhomogeneous Superconductivity in BaPb_{1-x}Bi_xO₃*, J. Supercond. Nov. Magn. **26**, 2675 (2013).
- ¹⁷ Y. Hidaka, M. Suzuki, T. Murakami, and T. Inamura, *Effects of a lead oxide annealing atmosphere on the superconducting properties of BaPb_{0.7}Bi_{0.3}O₃ sputtered films*, Thin Solid Films **106**, 311 (1983).
- ¹⁸ T. Takagi, Y.-M. Chiang, and A. Roshko, *Origin of grain boundary weak links in BaPb_{1-x}Bi_xO₃ superconductor*, J. Appl. Phys. **68**, 5750 (1990).
- ¹⁹ I. Roshchin, V. Stepankin, and A. Kuznetsov, *Reentrant superconducting transport behavior of single grain boundary Josephson junction in BaPb_{1-x}Bi_xO₃ Bicrystals*, J. Low Temp. Phys. **100**, 229 (1995).
- ²⁰ V. F. Gantmakher and V. T. Dolgoplov, *Superconductor-insulator quantum phase transition*, Phys.-Uspekhi **53**, 1 (2010).
- ²¹ Y.-H. Lin, J. Nelson, and A. M. Goldman, *Superconductivity of very thin films: The superconductor-insulator transition*, Phys. C Supercond. Its Appl. **514**, 130 (2015).
- ²² A. M. Finkel'stein, *Suppression of superconductivity in homogeneously disordered systems*, Phys. B Condens. Matter **197**, 636 (1994).
- ²³ G. Kim, M. Neumann, M. Kim, M. D. Le, T. D. Kang, and T. W. Noh, *Suppression of Three-Dimensional Charge Density Wave Ordering via Thickness Control*, Phys. Rev. Lett. **115**, 226402 (2015).

- ²⁴ B. Meir, S. Gorol, T. Kopp, and G. Hammerl, *Observation of two-dimensional superconductivity in bilayers of BaBiO₃ and BaPbO₃*, Phys. Rev. B **96**, 100507 (2017).
- ²⁵ S. H. Oh and C. G. Park, *Misfit strain relaxation by dislocations in SrRuO₃/SrTiO₃ (001) heteroepitaxy*, J. Appl. Phys. **95**, 4691 (2004).
- ²⁶ G. Gao, S. Jin, and W. Wu, *Lattice-mismatch-strain induced inhomogeneities in epitaxial La_{0.7}Ca_{0.3}MnO₃ films*, Appl. Phys. Lett. **90**, 012509 (2007).
- ²⁷ C. J. M. Daumont, D. Mannix, S. Venkatesan, G. Catalan, D. Rubi, B. J. Kooi, J. T. M. D. Hosson, and B. Noheda, *Epitaxial TbMnO₃ thin films on SrTiO₃ substrates: a structural study*, J. Phys. Condens. Matter **21**, 182001 (2009).
- ²⁸ H. Yamahara, M. Mikami, M. Seki, and H. Tabata, *Epitaxial strain-induced magnetic anisotropy in Sm₃Fe₅O₁₂ thin films grown by pulsed laser deposition*, J. Magn. Magn. Mater. **323**, 3143 (2011).
- ²⁹ See Supplementary Materials file for further details.
- ³⁰ E. Climent-Pascual, N. Ni, S. Jia, Q. Huang, and R. J. Cava, *Polymorphism in BaPb_{1-x}Bi_xO₃ at the superconducting composition*, Phys. Rev. B **83**, 174512 (2011).
- ³¹ Y. Ivry, C.-S. Kim, A. E. Dane, D. De Fazio, A. N. McCaughan, K. A. Sunter, Q. Zhao, and K. K. Berggren, *Universal scaling of the critical temperature for thin films near the superconducting-to-insulating transition*, Phys. Rev. B **90**, 214515 (2014).
- ³² M. D. Biegalski, D. D. Fong, J. A. Eastman, P. H. Fuoss, S. K. Streiffer, T. Heeg, J. Schubert, W. Tian, C. T. Nelson, X. Q. Pan, M. E. Hawley, M. Bernhagen, P. Reiche, R. Uecker, S. Trolier-McKinstry, and D. G. Schlom, *Critical thickness of high structural quality SrTiO₃ films grown on orthorhombic (101) DyScO₃*, J. Appl. Phys. **104**, 114109 (2008).
- ³³ V. Darakchieva, J. Birch, M. Schubert, T. Paskova, S. Tungasmita, G. Wagner, A. Kasic, and B. Monemar, *Strain-related structural and vibrational properties of thin epitaxial AlN layers*, Phys. Rev. B **70**, 045411 (2004).
- ³⁴ J. M. Ziman, *Models of Disorder: The Theoretical Physics of Homogeneously Disordered Systems* (Cambridge university Press, New York, 1979).
- ³⁵ B. Kramer and A. MacKinnon, *Localization: theory and experiment*, Rep. Prog. Phys. **56**, 1469 (1993).
- ³⁶ Y. P. Timalisina, A. Horning, R. F. Spivey, K. M. Lewis, T.-S. Kuan, G.-C. Wang, and Toh-Ming Lu, *Effects of nanoscale surface roughness on the resistivity of ultrathin epitaxial copper films*,

- Nanotechnology **26**, 075704 (2015).
- ³⁷ A. Larkin and A. Varlamov, *Theory of Fluctuations in Superconductors*, (Oxford University Press, Oxford, 2005).
- ³⁸ T. I. Baturina, A. Yu. Mironov, V. M. Vinokur, M. R. Baklanov, and C. Strunk, *Localized Superconductivity in the Quantum-Critical Region of the Disorder-Driven Superconductor-Insulator Transition in TiN Thin Films*, Phys. Rev. Lett. **99**, 257003 (2007).
- ³⁹ M. Chand, G. Saraswat, A. Kamlapure, M. Mondal, S. Kumar, J. Jesudasan, V. Bagwe, L. Benfatto, V. Tripathi, and P. Raychaudhuri, *Phase diagram of the strongly disordered s-wave superconductor NbN close to the metal-insulator transition*, Phys. Rev. B **85**, 014508 (2012).
- ⁴⁰ A. Larkin, *Superconductor-insulator transitions in films and bulk materials*, Ann. Phys. **8**, 785 (1999).
- ⁴¹ M. D. Stewart, Jr., Aijun Yin, J. M. Xu, and J. M. Valles, Jr., *Magnetic-field-tuned superconductor-to-insulator transitions in amorphous Bi films with nanoscale hexagonal arrays of holes*, Phys. Rev. B **77**, 140501(R) (2008).
- ⁴² G. Kopnov, O. Cohen, M. Ovadia, K. Hong Lee, C. C. Wong, and D. Shahar, *Little-Parks Oscillations in an Insulator*, Phys. Rev. Lett. **109**, 167002 (2012).
- ⁴³ I. Shammass, O. Cohen, M. Ovadia, I. Gutman, and D. Shahar, *Superconducting correlations in thin films of amorphous indium oxide on the insulating side of the disorder-tuned superconductor-insulator transition*, Phys. Rev. B **85**, 140507(R).
- ⁴⁴ G. Bergmann, *Quantum corrections to the resistance in two-dimensional disordered superconductors above T_c : Al, Sn, and amorphous $Bi_{0.9}Tl_{0.1}$ films*, Phys. Rev. B **29**, 6114 (1984).
- ⁴⁵ James M. Gordon and A. M. Goldman, *Electron inelastic scattering in aluminum films and wires at temperatures near the superconducting transition*, Phys. Rev. B **34**, 1500 (1986).
- ⁴⁶ B. Shinozaki and L. Rinderer, *Temperature and randomness dependence of the pair-breaking parameter in superconducting aluminum films*, J. Low Temp. Phys. **73**, 267 (1988).
- ⁴⁷ M. Giannouri, E. Rocofyllou, C. Papastaikoudis, and W. Schilling, *Weak-localization, Aslamazov-Larkin, and Maki-Thompson superconducting fluctuation effects in disordered $Zr_{1-x}Rh_x$ films above T_c* , Phys. Rev. B **56**, 6148 (1997).
- ⁴⁸ A. Glatz, A. A. Varlamov, and V. M. Vinokur, *Fluctuation spectroscopy of disordered two-dimensional superconductors*, Phys. Rev. B **84**, 104510 (2011).
- ⁴⁹ Brian Tarasinski and Georg Schwiete, *Fluctuation conductivity of disordered superconductors in*

- magnetic fields*, Phys. Rev. B **88**, 014518 (2013).
- ⁵⁰ Alex Levchenko, *Magnetoconductivity of low-dimensional disordered conductors at the onset of the superconducting transition*, Phys. Rev. B **79**, 212511 (2009).
- ⁵¹ R. Rosenbaum, S.-Y. Hsu, J.-Y. Chen, Y.-H. Lin, and J.-J. Lin, *Superconducting fluctuation magnetoconductance in a tungsten carbide film*, J. Phys. Condens. Matter **13**, 10041 (2001).
- ⁵² B. Batlogg, *Superconductivity in $Ba(Pb,Bi)O_3$* , Phys. BC **126**, 275 (1984).
- ⁵³ P. Giraldo-Gallo, Y. Zhang, C. Parra, H. C. Manoharan, M. R. Beasley, T. H. Geballe, M. J. Kramer, and I. R. Fisher, *Stripe-like nanoscale structural phase separation in superconducting $BaPb_{1-x}Bi_xO_3$* , Nat. Commun. **6**, 8231 (2015).
- ⁵⁴ A. Chainani, T. Yokoya, T. Kiss, S. Shin, T. Nishio, and H. Uwe, *Electron-phonon coupling induced pseudogap and the superconducting transition in $Ba_{0.67}K_{0.33}BiO_3$* , Phys. Rev. B **64**, 180509 (2001).
- ⁵⁵ K. Kitazawa, S. Uchida, and S. Tanaka, *A new density of states model of $BaPb_{1-x}Bi_xO_3$* , Phys. BC **135**, 505 (1985).
- ⁵⁶ S. Tajima, S. Uchida, A. Masaki, H. Takagi, K. Kitazawa, S. Tanaka, and A. Katsui, *Optical study of the metal-semiconductor transition in $BaPb_{1-x}Bi_xO_3$* , Phys. Rev. B **32**, 6302 (1985).
- ⁵⁷ D. Nicoletti, E. Casandruc, D. Fu, P. Giraldo-Gallo, I. R. Fisher, and A. Cavalleri, *Anomalous relaxation kinetics and charge-density-wave correlations in underdoped $BaPb_{1-x}Bi_xO_3$* , Proc. Natl. Acad. Sci. **114**, 9020 (2017).
- ⁵⁸ D. T. Marx, P. G. Radaelli, J. D. Jorgensen, R. L. Hitterman, D. G. Hinks, S. Pei, and B. Dabrowski, *Metastable behavior of the superconducting phase in the $BaBi_{1-x}Pb_xO_3$* , Phys. Rev. B **46**, 1144 (1992).
- ⁵⁹ H. Y. Hwang, Y. Iwasa, M. Kawasaki, B. Keimer, N. Nagaosa, and Y. Tokura, *Emergent phenomena at oxide interfaces*, Nat. Mater. **11**, 103 (2012).
- ⁶⁰ J. Chakhalian, A. J. Millis, and J. Rondinelli, *Whither the oxide interface*, Nat. Mater. **11**, 92 (2012).
- ⁶¹ B. Yan, M. Jansen, and C. Felser, *A large-energy-gap oxide topological insulator based on the superconductor $BaBiO_3$* , Nat. Phys. **9**, 709 (2013).